The Astrophysical Journal, 627:L33–L36, 2005 July 1

# *SPITZER* OBSERVATIONS OF $CO_2$ ICE TOWARD FIELD STARS IN THE TAURUS MOLECULAR CLOUD

Edwin A. Bergin,[1] Gary J. Melnick,[2] Perry A. Gerakines,[3] David A. Neufeld,[4] and Douglas C. B. Whittet[5]

*Received 2005 February 24; accepted 2005 May 16; published 2005 June 8*

## ABSTRACT

We present the first *Spitzer* Infrared Spectrograph observations of the 15.2 $\mu$m bending mode of $CO_2$ ice toward field stars behind a quiescent dark cloud. $CO_2$ ice is detected toward two field stars (Elias 16 and Elias 3) and a single protostar (HL Tau) with an abundance of ∼15%–20% relative to water ice. $CO_2$ ice is not detected toward the source with lowest extinction in our sample, Tamura 17 ($A_V = 3.9$ mag). A comparison of the Elias 16 spectrum with laboratory data demonstrates that the majority of $CO_2$ ice is embedded in a polar, $H_2O$-rich ice component, with ∼15% of $CO_2$ residing in an apolar, $H_2O$-poor mantle. This is the first detection of apolar $CO_2$ toward a field star. We find that the $CO_2$ extinction threshold is $A_V = 4 \pm 1$ mag, comparable to the threshold for water ice, but significantly less than the threshold for CO ice, the likely precursor of $CO_2$. Our results confirm that $CO_2$ ice forms in tandem with $H_2O$ ice along quiescent lines of sight. This argues for $CO_2$ ice formation by means of a mechanism similar to that responsible for $H_2O$ ice formation, viz., simple catalytic reactions on grain surfaces.

*Subject headings:* astrobiology — astrochemistry — ISM: lines and bands — ISM: molecules

## 1. INTRODUCTION

Observations by the *Infrared Space Observatory* (*ISO*) have demonstrated that $CO_2$ ice is a ubiquitous component of the interstellar medium (ISM), with typical abundance of ∼15%–25% relative to $H_2O$, the dominant ice component (Gerakines et al. 1999; Nummelin et al. 2001). However, the origin of this common grain-mantle constituent remains uncertain. Gas-phase production, with subsequent freeze-out, is believed incapable of reproducing the observed abundance. In the laboratory, $CO_2$ forms quite readily via UV photolysis or ion bombardment of astrophysical ice mixtures; along with the thermal processing of ices, these mechanisms have been suggested as possible formation routes (d'Hendecourt et al. 1986; Sandford et al. 1988; Palumbo et al. 1998). Even if UV photons and cosmic rays are not present with sufficient fluxes, an alternative mechanism is grain surface chemistry (Roser et al. 2001; Frost et al. 1991 and references therein). Observations of grain mantles indicate that there is competition between hydrogenation and oxidation of atoms on grain surfaces (van Dishoeck 2004 and references therein). Nowhere is this more clear than for carbon-bearing molecules. $CO_2$ ice is less volatile than CO (Sandford & Allamandola 1990), and its formation locks carbon in saturated form on grains, stopping any subsequent hydrogenation toward more complex molecules on grains or in the gas. Thus, an understanding of the formation mechanisms of $CO_2$ ice is needed in order to understand the limits of grain surface chemistry in producing more complex organics.

One way to constrain the origin of $CO_2$ ice in the ISM is to use bright field stars located behind molecular cloud material as candles that probe material remote from embedded sources, where, at suitably high extinction, ices are unlikely to be exposed to significant UV radiation or heating. *ISO* detected the $CO_2$ 4.27 $\mu$m $\nu_3$ stretching mode toward only two K giants, Elias 13 and 16 (Whittet et al. 1998; Nummelin et al. 2001). However, the detection of $CO_2$ ice toward any field star demonstrated that radiative processing of ices is unlikely to be responsible for the $CO_2$ ice production in quiescent material (Whittet et al. 1998).

In this Letter, we report and discuss the implications of the observation of the $\nu_2$ bending mode of $CO_2$ ice at 15.2 $\mu$m toward three field stars and one protostar in the Taurus molecular cloud using NASA's *Spitzer Space Telescope*.

## 2. OBSERVATIONS AND RESULTS

Observations of each source (see Table 1) were obtained in 2004 using the *Spitzer* Infrared Spectrograph (IRS; Houck et al. 2004). Each object was observed in staring mode in the short-wavelength, high-resolution module ("Short-High"), which has coverage from 10 to 19 $\mu$m with $\lambda/\Delta\lambda \sim 600$. Each exposure was taken using a per-cycle integration time of 120 s with four cycles. All data were reduced using the IRS team's SMART program (Higdon et al. 2004), starting with data products from pipeline version 13. Our data reduction process mirrored that described by Watson et al. (2004; see § 2 in that paper).

Figure 1 shows the IRS spectra, with a clear $CO_2$ absorption feature at ∼15 $\mu$m for Elias 16, Elias 3, and HL Tau. For Tamura 17, the star tracing the lowest extinction in our sample (Table 1), the stellar continuum is detected but no absorption feature is observed. For $CO_2$, the 15 $\mu$m feature's optical depth is derived by fitting a multiorder polynomial to determine the continuum. In general, polynomials with orders 2–4 (higher order for Elias 16) were required to account for the mismatch in the continuum on the longward side of the $CO_2$ line caused by wings of the broad 18.5 $\mu$m silicate feature. Column densities are estimated using $N(CO_2) = \int \tau(\tilde{\nu})\Delta\tilde{\nu}/A_{15.2\,\mu m}$, where $\tilde{\nu}$ is the frequency in wavenumber units and a value of $10^{-17}$ cm per molecule is assumed for $A_{15.2\,\mu m}$ (Gerakines et al. 1995). The column density derived toward Elias 16 is identical, within errors, to that derived earlier by Whittet et al. (1998) using the *ISO* detection of the 4.27 $\mu$m line.

## 3. ELIAS 16 LINE PROFILE

The Elias 16 spectrum possesses a sufficient signal-to-noise ratio to permit an analysis of the ice composition (Gerakines

---

[1] Department of Astronomy, University of Michigan, 825 Dennison Building, 500 Church Street, Ann Arbor, MI 48109; ebergin@umich.edu.

[2] Harvard-Smithsonian Center for Astrophysics, 60 Garden Street, Cambridge, MA 02138.

[3] Astro- and Solar-System Physics Program, Department of Physics, University of Alabama at Birmingham, Birmingham, AL 35294-1170.

[4] Department of Physics and Astronomy, Johns Hopkins University, 3400 North Charles Street, Baltimore, MD 21218.

[5] Department of Physics, Applied Physics, and Astronomy, and New York Center for Studies on the Origins of Life, Rensselaer Polytechnic Institute, 110 Eighth Street, Troy, NY 12180.

TABLE 1

Observation Parameters and Results

| Source | Obs. Date (2004) | $\int \tau(\tilde{\nu})\Delta\tilde{\nu}$[a] | $N(CO_2)$[b] | $\frac{N(CO_2)}{N(H_2O)}$ | $\frac{N(CO_2)}{N(CO)}$ | $A_V$ |
|---|---|---|---|---|---|---|
| Elias 16[c] ........ | Mar 3 | 5.0 ± 0.1 | 5.0 | 0.21 | 0.8 | 23.3 |
| Elias 3[c] .......... | Mar 3 | 1.8 ± 0.1 | 1.8 | 0.20 | 1.0 | 10.0 |
| Tamura 17[c] ...... | Feb 27 | <0.1 (3 $\sigma$) | <0.12 | <0.10 | ... | 3.9 |
| HL Tau .......... | Oct 10 | 1.9 ± 0.1 | 1.9 | 0.14 | ... | 24.0 |

Note.—$N$(CO) data for field stars and the limiting value for HL Tau are from Chiar et al. (1995) and Tegler et al. (1995), respectively. The $A_V$ value for HL Tau is from Close et al. (1997); those for field stars are calculated from the $J-K$ color excess assuming $A_V = 5.3E_{J-K}$ (Whittet et al. 2001).

[a] For Elias 16, Elias 3, and HL Tau, integrated optical depths are calculated by a direct integration over the profile. For Tamura 17, we have estimated the opacity limit by fitting a series of Gaussians with fixed width and line center determined by the Elias 3 feature. The absorption depth is variable and the minimum optical depth that fits the noise is used to estimate the 3 $\sigma$ integrated opacity. Units are cm$^{-1}$.

[b] In units of $10^{17}$ cm$^{-2}$.

[c] Field star.

et al. 1999; Nummelin et al. 2001). The 4.27 $\mu$m feature detected by *ISO* constrained the majority of $CO_2$ to lie within a single polar ice component with $H_2O:CO_2:CO$ (100 : 20 : 3) at 20 K (Whittet et al. 1998). This contrasts with CO ice, which resides primarily in an apolar component (Chiar et al. 1995).

The $CO_2$ bending mode is more sensitive than the stretching mode to the ice composition (Ehrenfreund et al. 1996), and the spectrum, shown in Figure 2, exhibits clear asymmetry. We have used a similar set of laboratory interstellar ice analogs (Ehrenfreund et al. 1996, 1997) with a $\chi^2$ minimization routine (Gerakines et al 1999) to constrain the ice composition. Because the gas temperature of the Taurus cloud is ~10 K, we only present fits using ice analogs at 10 K and have excluded any spectra that include appreciable amounts of $O_2$. Molecular oxygen has yet to be detected in the ISM either by direct detection in the gas phase or by indirect methods on grain surfaces (Vandenbussche et al. 1999; Goldsmith et al. 2000; Pagani et al. 2003).

Our best fit (Fig. 2) requires two components, a broad feature consistent with $CO_2$ ice within the polar water mantle ($H_2O$ : $CO_2$ 100 : 14) and a narrow component of $CO_2$ embedded in an apolar matrix ($CO:CO_2$ 100 : 26). The majority of $CO_2$ resides in the polar component, while apolar $CO_2$ ice accounts for ~15% of the $CO_2$ ice column.[6]

## 4. ICE EXTINCTION THRESHOLD

It is known from previous studies of ice features in Taurus that the absorption strength correlates with extinction. The correlation line intercepts the extinction axis at a positive value; that is, there exists a threshold extinction below which the ice feature is not seen, presumably because the grains in the more diffuse outer layers of the cloud are not mantled (see, e.g., Chiar et al. 1995; Whittet et al. 2001 and references therein). Figure 3 compares plots of column density versus extinction for $CO_2$ and CO. In the case of $CO_2$, we combine both *Spitzer* and *ISO* observations. The field star data suggest a correlation yielding a threshold extinction $A_V = 4 \pm 1$ mag, that is, not significantly different from the value of 3.2 ± 0.1 mag reported for water ice (Whittet et al. 2001). In contrast, the threshold estimated for CO (6.8 ± 1.6 mag) appears to be significantly larger. These results are consistent with a model in which most of the $CO_2$ is in the polar, $H_2O$-rich component, whereas most of the CO is in the apolar, $H_2O$-poor component. A larger threshold is expected for the latter because of its greater volatility, requiring a greater degree of screening from the external radiation field.[7]

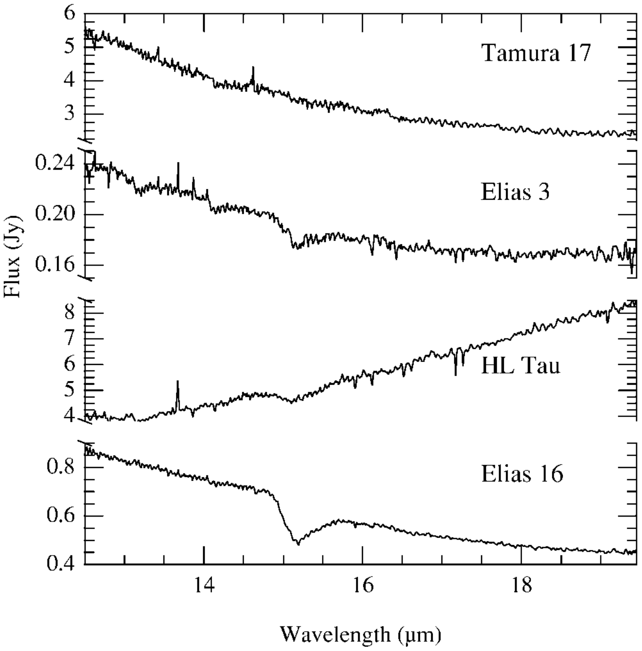

Fig. 1.—*Spitzer* IRS Short-High spectra toward background stars Tamura 17, Elias 3, and Elias 16; HL Tau is a Class I pre–main-sequence star. These spectra are shown without any baseline subtraction.

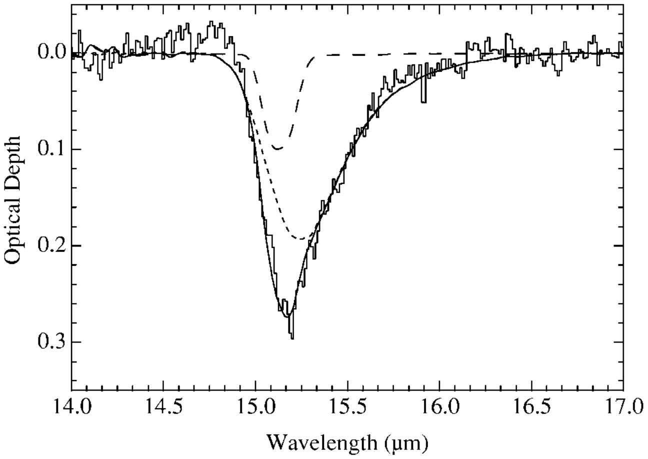

Fig. 2.—Optical depth of $CO_2$ ice absorption seen toward Elias 16 (*histogram*) and best-fit line profile using laboratory analogs of interstellar ice mixtures at 10 K (*solid line*). The best fit requires two components: $CO_2$ embedded in a water-rich (polar) mantle, shown as the short-dashed line (laboratory ice analog mixture $H_2O + CO_2$, 100 : 14). The second component, shown as a long-dashed line, is $CO_2$ embedded in an apolar mantle (laboratory ice analog mixture $CO + CO_2$, 100 : 26).

---

[6] This apolar component is effectively hidden within the *ISO* 4.27 $\mu$m spectrum of Elias 16, as there is little difference in the fits obtained with a purely polar mixture (Whittet et al. 1998) and those including a weak apolar component such as that found here.

[7] Note that the pre–main-sequence star HL Tau does not follow the field star trend in either panel of Fig. 3. Much of the extinction toward this object evidently arises in a circumstellar disk (e.g., Close et al. 1997). Temperatures in the disk likely range from ~100 K, where CO is entirely in the gas phase (see Gibb et al. 2004b), to much higher temperatures where all ice mantles are sublimated. That $CO_2$ is detectable in solid form toward HL Tau is consistent with its residence in a polar matrix.

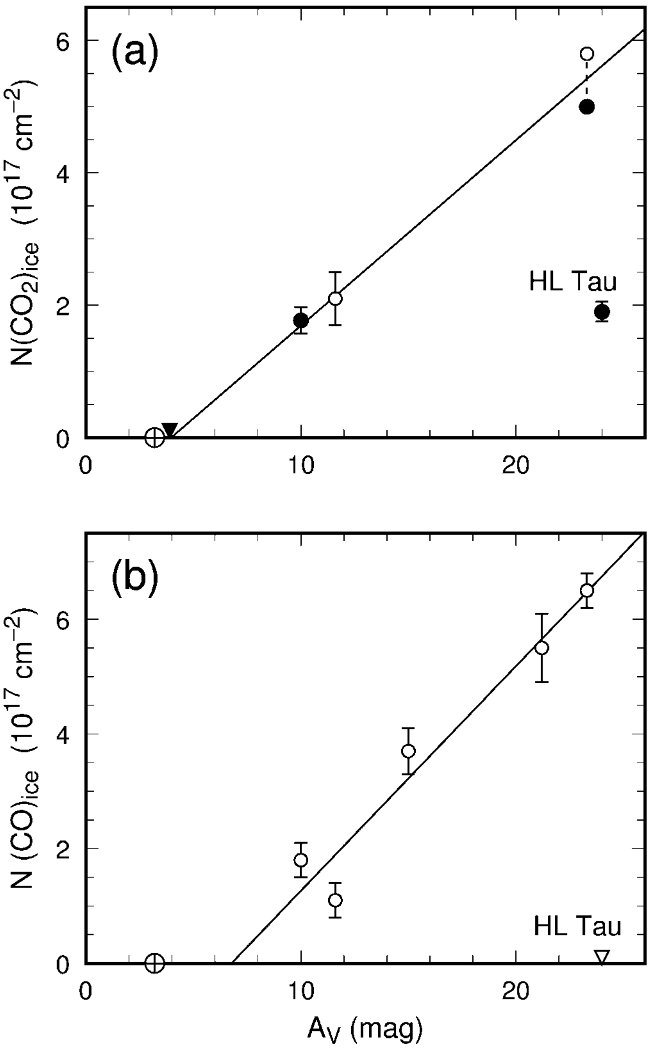

FIG. 3.—Plots of ice column density vs. visual extinction for (*a*) $CO_2$ and (*b*) CO. Open and filled symbols in (*a*) represent stretching and bending vibrational modes of $CO_2$, observed with the *ISO* SWS (Gerakines et al. 1999; Nummelin et al. 2001) and *Spitzer* IRS (this paper), respectively. The points for one object (Elias 16) observed in both vibrational modes are joined by a vertical dashed line. Triangles indicate upper limits. The circled plus sign on the $A_V$ axis indicates the locus of the threshold extinction for $H_2O$ ice ($A_V$ = 3.2; Whittet et al. 2001). The diagonal line in each panel is the linear least-squares fit to field stars.

Figure 4 plots ice-phase column densities for $CO_2$ versus $H_2O$ and CO. In the case of $CO_2$ versus $H_2O$, there is a general trend—linear least-squares fits to field stars and young stellar objects (YSOs) are similar and intercept close to the origin. In contrast, the $CO_2$ versus CO plot shows a tendency to divide into two distinct trends (Gerakines et al. 1999). For a given CO ice column, field stars have a lower $CO_2$ ice column than massive YSOs. Grains in front of field stars are covered by polar and apolar mantles. In contrast, in the warm envelopes of massive YSOs, the dominant factor is likely to be sublimation of apolar CO-rich ices (although some $CO_2$ might also be produced by energetic processes). The lower mass YSOs show an intermediate distribution.

## 5. IMPLICATIONS FOR $CO_2$ ICE FORMATION

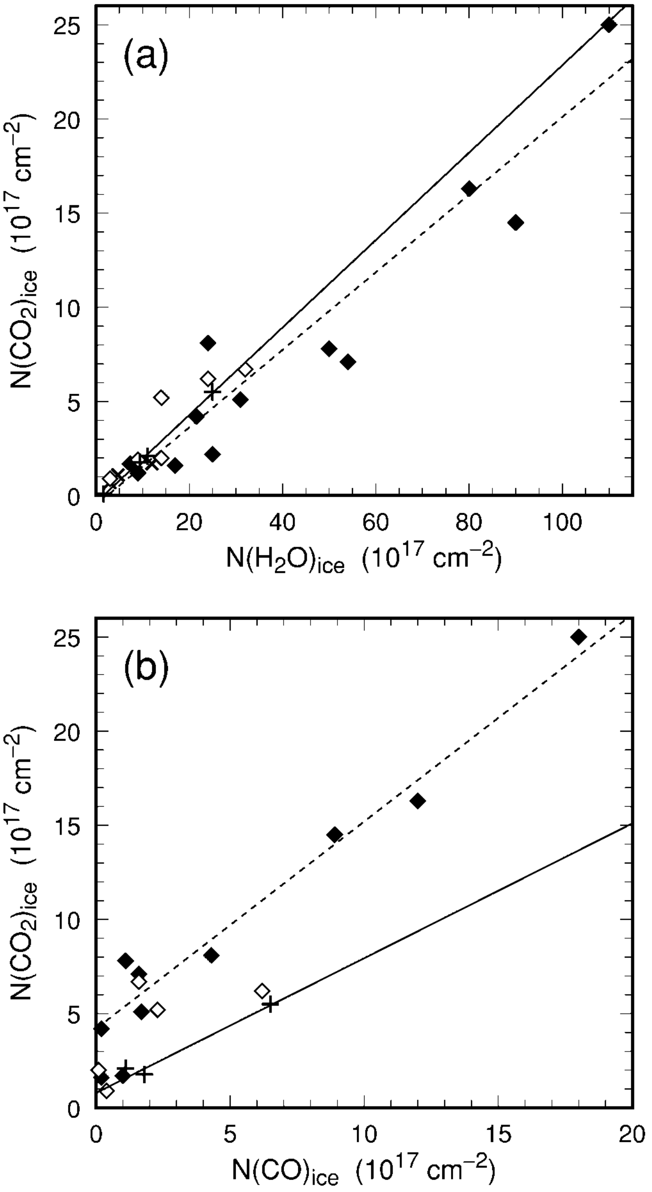

FIG. 4.—Plots of $N(CO_2)$ vs. (*a*) $N(H_2O)$ and (*b*) $N$(CO) for all sources with data available from *Spitzer* (this paper) or the *ISO* SWS (Gerakines et al. 1999; Nummelin et al. 2001): *plus signs*, Taurus field stars; *crosses*, Galactic center field stars; *open diamonds*, low-mass YSOs; *filled diamonds*, high-mass YSOs. The solid diagonal line in each panel is the linear least-squares fit to field stars. The dashed line in (*a*) is the fit to YSOs only (both high and low mass). The dashed line in (*b*) is the relation $N(CO_2) = (4.2 \times 10^{17}) + 1.1N(CO)$ proposed by Gerakines et al. (1999) for high-mass YSOs.

The *Spitzer* data on field stars revealed that (1) most of the $CO_2$ ice is embedded within the water ice mantle and (2) the $CO_2$ extinction threshold is closer to the threshold for water ice than that of its presumed precursor molecule, CO. These two results strongly suggest that $CO_2$ ice formation occurs in tandem with that of water ice. Water ice is believed to form by means of surface reactions during phases when gas is rich in atomic hydrogen and atomic oxygen. Observations of water vapor imply that atomic oxygen must be depleted in dense, evolved, well-shielded molecular regions; the low abundance of gas-phase water inferred by *SWAS* (Snell et al. 2000) and *Odin* (Olofsson et al. 2003) can only be accounted for in models where nearly all available gas-phase atomic oxygen becomes locked on grains (Bergin et al. 2000).

Thus, $H_2O$ and $CO_2$ ice formation must occur during the early, lower density formative stages of the cloud. Recent models of molecular cloud formation behind shock waves by Bergin et al. (2004) may therefore be useful in setting constraints on ice formation. They found that $H_2$ formation occurs at earlier times than gas-phase CO formation because $H_2$ efficiently self-shields, while CO formation requires dust shielding ($A_V \sim 0.7$ mag). At such low cloud depths, ice mantle formation would be retarded by UV photodesorption. However, for $A_V > 1.0$ mag the effects of photodesorption are greatly reduced. In this scenario, CO gas-phase formation precedes both CO and water ice mantle formation. This qualitatively answers several questions. Because most available gas-phase carbon would be locked in gas-phase CO, it would preclude a high abundance of methane ice, in accord with observations (Gibb et al. 2004a). It also allows for H, O, and CO to be present on the grain surface to react by means of simple catalytic reactions to create $H_2O$ and $CO_2$.[8]

One key question remains: How to account for the presence of apolar $CO_2$ ice? If $CO_2$ forms in tandem with $H_2O$ in oxygen-rich gas, then how is a separate component of $CO_2$ formed with little $H_2O$? This implies the presence of O I in gas with little H I. There are at least two scenarios that could account for this mantle structure: line-of-sight structure in the abundance of atomic hydrogen, or in atomic oxygen (or perhaps both). To examine the question of line-of-sight structure in atomic hydrogen, in Elias 16 the abundance of $CO_2$ in the apolar mantle is $\sim 3 \times 10^{-6}$ (all abundances relative to $H_2$): thus, gas-phase H I would need to fall below this value to stop O I hydrogenation. Atomic hydrogen is expected to have near-constant space density in molecular clouds, $n_{\rm H\,I} \sim 1$–$5$ cm$^{-3}$ (see Goldsmith & Li 2005). Thus, the H I abundance should inversely follow density variations along the Elias 16 line of sight. However, the density would need to be over $10^6$ cm$^{-3}$ for the abundance of H I to fall below that required for O I. This density is characteristic of a condensed molecular core, which is not detected toward this line of sight (Cernicharo & Guélin 1987), and is therefore implausibly high. Thus, H I abundance structure is insufficient to account for apolar $CO_2$.

Line-of-sight structure in the O I abundance provides a more plausible solution to this issue. If atomic oxygen were absent in the densest regions with high extinction, by water ice formation and other additional solid-state reservoirs, then oxygen hydrogenation could have halted in these regions. Oxidation could continue in layers with lower extinction and density. For instance, assuming a density of $10^4$ cm$^{-3}$ for the Elias 16 line of sight (Bergin et al. 1995), the atomic oxygen abundance would need to be $\gtrsim 10^{-4}$ to be higher than H I, which is conceivable given the available O I ($\sim 8 \times 10^{-4}$; Jensen et al. 2005). Thus, CO oxidation could continue in outer layers rich in atomic oxygen. There is some evidence for large O I columns toward molecular clouds that may trace low-density layers (Caux et al. 1999; Lis et al. 2001; Li et al. 2002 and references therein). This qualitative model can be tested by future higher signal-to-noise ratio *Spitzer* observations of low-extinction field stars (e.g., Elias 3). For instance, line-of-sight structure in the oxygen abundance would predict the existence of apolar $CO_2$ at moderate optical depths, even at those below the CO ice threshold. Alternately, under the assumption that lower $A_V$ implies lower density, decreasing amounts of apolar $CO_2$ would suggest a relation to the declining abundance of atomic hydrogen with increasing density.

We are grateful to the referee for useful comments. D. C. B. W. acknowledges financial support from the NASA NSCORT program (grant NAG 5-12750), and D. A. N. gratefully acknowledges support from NASA's LTSA program. This work is based on observations made with the *Spitzer Space Telescope*, which is operated by JPL/Caltech under NASA contract 1407. We are grateful to D. Watson and J. Green for aid in the data reduction and are thankful for support from G. Fazio and the IRAC team. These observations were performed as part of the IRAC Guaranteed Time Observations program.

[8] $CH_3OH$ ice is not detected toward field stars (Chiar et al. 1996). Thus, observations would suggest that grain surface formation of $CH_3OH$ is inefficient under low-temperature quiescent conditions. Laboratory experiments investigating the hydrogenation sequence for CO, $CO \rightarrow HCO \rightarrow H_2CO \rightarrow CH_3OH$ (excluding some intermediate products) are discussed by Hiraoka et al. (2005 and references therein).

## REFERENCES

Bergin, E. A., Hartmann, L. W., Raymond, J. C., & Ballesteros-Paredes, J. 2004, ApJ, 612, 921
Bergin, E. A., Langer, W. D., & Goldsmith, P. F. 1995, ApJ, 441, 222
Bergin, E. A., et al. 2000, ApJ, 539, L129
Caux, E., et al. 1999, A&A, 347, L1
Cernicharo, J., & Guélin, M. 1987, A&A, 176, 299
Chiar, J. E., Adamson, A. J., Kerr, T. H., & Whittet, D. C. B. 1995, ApJ, 455, 234
Chiar, J. E., Adamson, A. J., & Whittet, D. C. B. 1996, ApJ, 472, 665
Close, L. M., Roddier, F., Northcott, M. J., Roddier, C., & Graves, J. E. 1997, ApJ, 478, 766
d'Hendecourt, L. B., Allamandola, L. J., Grim, R. J. A., & Greenberg, J. M. 1986, A&A, 158, 119
Ehrenfreund, P., Boogert, A. C. A., Gerakines, P. A., Jansen, D. J., Schutte, W. A., Tielens, A. G. G. M., & van Dishoeck, E. F. 1996, A&A, 315, L341
Ehrenfreund, P., Boogert, A. C. A., Gerakines, P. A., Tielens, A. G. G. M., & van Dishoeck, E. F. 1997, A&A, 328, 649
Frost, M. J., Sharkey, P., & Smith, I. W. M. 1991, Faraday Discuss. Chem. Soc., 91, 305
Gerakines, P. A., Schutte, W. A., Greenberg, J. M., & van Dishoeck, E. F. 1995, A&A, 296, 810
Gerakines, P. A., et al. 1999, ApJ, 522, 357
Gibb, E. L., Rettig, T., Brittain, S., Haywood, R., Simon, T., & Kulesa, C. 2004a, ApJ, 610, L113
Gibb, E. L., Whittet, D. C. B., Boogert, A. C. A., & Tielens, A. G. G. M. 2004b, ApJS, 151, 35
Goldsmith, P. F., & Li, D. 2005, ApJ, 622, 938
Goldsmith, P. F., et al. 2000, ApJ, 539, L123
Higdon, S. J. U., et al. 2004, PASP, 116, 975
Hiraoka, K., et al. 2005, ApJ, 620, 542
Houck, J. R., et al. 2004, ApJS, 154, 18
Jensen, A. G., Rachford, B. L., & Snow, T. P. 2005, ApJ, 619, 891
Li, W., Evans, N. J., II, Jaffe, D. T., van Dishoeck, E. F., & Thi, W.-F. 2002, ApJ, 568, 242
Lis, D. C., Keene, J., Phillips, T. G., Schilke, P., Werner, M. W., & Zmuidzinas, J. 2001, ApJ, 561, 823
Nummelin, A., Whittet, D. C. B., Gibb, E. L., Gerakines, P. A., & Chiar, J. E. 2001, ApJ, 558, 185
Olofsson, A. O. H., et al. 2003, A&A, 402, L47
Pagani, L., et al. 2003, A&A, 402, L77
Palumbo, M. E., Baratta, G. A., Brucato, J. R., Castorina, A. C., Satorre, M. A., & Strazzulla, G. 1998, A&A, 334, 247
Roser, J. E., Vidali, G., Manicò, G., & Pirronello, V. 2001, ApJ, 555, L61
Sandford, S. A., & Allamandola, L. J. 1990, Icarus, 87, 188
Sandford, S. A., Allamandola, L. J., Tielens, A. G. G. M., & Valero, G. J. 1988, ApJ, 329, 498
Snell, R. L., et al. 2000, ApJ, 539, L101
Tegler, S. C., Weintraub, D. A., Rettig, T. W., Pendleton, Y. J., Whittet, D. C. B., & Kulesa, C. A. 1995, ApJ, 439, 279
Vandenbussche, B., et al. 1999, A&A, 346, L57
van Dishoeck, E. F. 2004, ARA&A, 42, 119
Watson, D. M., et al. 2004, ApJS, 154, 391
Whittet, D. C. B., Gerakines, P. A., Hough, J. H., & Shenoy, S. S. 2001, ApJ, 547, 872
Whittet, D. C. B., et al. 1998, ApJ, 498, L159